Actininopathy-a new muscular dystrophy caused by *ACTN2* dominant mutations

Journal:	*Annals of Neurology*
Manuscript ID	ANA-18-1305.R1
Wiley - Manuscript type:	Research Article
Date Submitted by the Author:	n/a
Complete List of Authors:	Savarese, Marco; Folkhälsan Institute of Genetics, University of Helsinki, Medicum Palmio, Johanna; University of Tampere, Neuromuscular Research Unit Poza, Juan José ; Hospital Universitario Donostia. San Sebastián. Spain, Department of Neurology Weinberg, Jan; Karolinska University Hospital, 141 86 Stockholm, Sweden Olivé, Montse; Hospital de Bellvitge, Institut de Neuropatologia Cobo Esteban, Anamaria; Centre de Compétences Maladies Neuromusculaires. Hôpital Marin APHP. Hendaye. France Vihola, Anna; Folkhälsan Institute of Genetics, Haartman Institute, University of Helsinki, Department of Medical Genetics Jonson, Per Harald; Folkhälsan Institute of Genetics and University of Helsinki, Sarparanta, Jaakko; Folkhälsan Institute of Genetics, Dept. of Medical Genetics, University of Helsinki Garcia Bragado, Federico; Hospital Universitario Donostia. San Sebastián. Spain, Department of Neurology URTIZBEREA, Andoni; Centre de Compétences Maladies Neuromusculaires. Hôpital Marin APHP. Hendaye. France Hackman, Peter; Folkhälsan Institute of Genetics, University of Helsinki, Dept.of Medical Genetics Udd, Bjarne; Vasa Central Hospital, Neurology; University of Helsinki, Folkhalsan Genetic Institute
Keywords:	ACTN2, distal myopathy, muscular dystrophy
Domain:	Immunology and/or Genetics

Title: **Actininopathy – a new muscular dystrophy caused by *ACTN2* dominant mutations**

Running head: ***ACTN2* mutations cause a new muscular dystrophy**

Marco Savarese PhD[1,2]*, Johanna Palmio MD, PhD[3]*, Juan José Poza MD, PhD[4], Jan Weinberg MD[5], Montse Olive MD, PhD[6], Ana Maria Cobo PhD[7], Anna Vihola PhD[1,2], Per Harald Jonson PhD[1,2], Jaakko Sarparanta PhD[1,2], Federico García-Bragado MD[4], Jon Andoni Urtizberea MD[7], Peter Hackman PhD[1,2], Bjarne Udd MD, PhD[1,2,3,8]

1 Folkhälsan Research Center, Helsinki, Finland;
2 Medicum, University of Helsinki, Finland;
3 Neuromuscular Research Center, Tampere University Hospital and Tampere University, Finland;
4 Department of Neurology. Hospital Universitario Donostia, San Sebastián. Spain;
5 Department of Neurology, Karolinska University Hospital, 141 86 Stockholm, Sweden.
6 Department of Pathology, Neuropathology and Neuromuscular Unit, IDIBELL-Hospital de Bellvitge, Hospitalet de Llobregat, Barcelona, Spain
7 Centre de Compétences Maladies Neuromusculaires. Hôpital Marin APHP. Hendaye. France
8 Department of Neurology, Vaasa Central Hospital, Finland.

Correspondence to:
J. Palmio, Department of Neurology, Neuromuscular Research Center, Tampere University Hospital and Tampere University, FIN-33014 Tampere University, Finland
Tel: +358-3-3116111
fax: +358-3-35516164
E-mail: johanna.palmio@uta.fi

number of characters in the Title:76
number of characters in the Running head:46
number of words in the Abstract: 132
number of words in the Introduction: 255
number of words in the Discussion: 717
number of words in the body of the manuscript: 2612
number of figures:6
number of color figures: 2
number of tables: 1

Abstract

Objective

To clinically and pathologically characterize a cohort of patients presenting with a novel form of distal myopathy and to identify the genetic cause of this new muscular dystrophy.

Methods

We studied four families (three from Spain and one from Sweden) suffering from an autosomal dominant distal myopathy. Affected members showed adult-onset asymmetric distal muscle weakness with initial involvement of ankle dorsiflexion later progressing also to proximal limb muscles.

Results

In all three Spanish families, we identified a unique missense variant in the *ACTN2* gene co-segregating with the disease. The affected members of the Swedish family carry a different *ACTN2* missense variant.

Interpretation

ACTN2 encodes for alpha actinin2 that is highly expressed in the sarcomeric Z-disk with a major structural and functional role. Actininopathy is thus a new genetically determined distal myopathy.

Keywords: ACTN2, distal myopathy, muscular dystrophy

Introduction

Distal myopathies, also called distal muscular dystrophies, are rare genetic diseases[1, 2], characterized by predominant weakness in the feet and/or hands, due to dystrophic degeneration of distal muscles in the lower, and less frequently, upper extremities[1, 2]. Although more than 20 different genes have been identified so far, a large number of patients do not harbor mutations in previously known disease genes[3].

Here we report four families with distal myopathy, sharing a similar clinical phenotype and a common pattern of muscle involvement. In all these families enrolled in the study, we identified missense variants in the alpha-actinin-2 gene (*ACTN2*, located on chromosome 1q43)[4] co-segregating with the disease.

ACTN2 mutations have previously been associated with both hypertrophic and dilated cardiomyopathies (HCM and DCM)[5, 6], but not with skeletal myopathies. Actinins are expressed in all human cells, they form dimeric filament cross-linking proteins[7]. Mammals have four genes encoding for slightly different proteins[7]. Alpha-actinin-2, in particular, is highly abundant in cardiac and skeletal muscle where it plays several functional and structural roles in the sarcomeres[7]. It is located in the Z-disk where it cross-links actin and titin filaments acting as a scaffold for other Z-disk proteins and also as a mechanosensor serving various signaling functions[7-9].

Despite the crucial role of alpha-actinin-2 and its interactions with other clinically relevant sarcomeric proteins[7, 9, 10], no *ACTN2* disease-causing mutations have been identified in patients with familial myopathies. During the preparation of our work we were aware of two sporadic patients with a different congenital progressive core myopathy being studied for *ACTN2*[11].

Materials and methods

Study subjects and clinical examinations

Four families with 18 patients affected by a distal myopathy of unknown genetic causes were investigated. Three families were from northern Spain (Families 1-3) and family 4 was from Sweden.

All the families showed an autosomal dominant inheritance pattern (Fig 1).

The patients had been clinically examined and most of them followed up over many years (Families 1, 2, and 4 for 8-15 years; family 3 for one year). Muscle imaging data, electrophysiological examination results (nerve conduction studies and needle electromyogram, EMG), creatine kinase (CK) measurements and cardiac function test results were obtained in most patients (Table 1).

All the patients provided written informed consent. The study was approved by Ethics Review Board of Helsinki University Hospital (number 195/13/03/00/11) and performed according to the Declaration of Helsinki.

Muscle biopsy

Muscle biopsies were obtained from five individuals and processed using standard histochemical reactions. Immunohistochemical analysis was performed using desmin (DakoCytomation, CloneD33) and myotilin (Novocastra, Clone RSO34) monoclonal antibodies. Moreover immunofluorescent (IF) stainings were performed using the following primary antibodies: monoclonal anti-alpha-actinin ACTN2/3 antibody (Sigma-Aldrich, clone EA-53); polyclonal anti-myotilin (ProteinTech 10731-1-AP); polyclonal anti–p62 (Millipore/Sigma P0067); and monoclonal anti-TDP-43 (Sigma-Aldrich WH0023435M1-1). Alexa-488 and Alexa-546 Fluor–conjugated secondary antibodies were used for detection, and Hoechst nuclear counterstain was performed prior to mounting in Fluoromount (Thermo Fisher Scientific).

A small sample of biopsies was fixed in 2% glutaraldehyde, postfixed with 1% osmium tetroxide, and embedded in araldite. Ultrathin sections were stained with uranyl acetate and lead citrate and viewed with a JEOL 1011 electron microscope.

Genetics

Genomic DNA was isolated from blood cells using standard techniques. DNA samples from the probands of Families 1,2 and 4 were sequenced using MYOcap, a targeted high-throughput sequencing panel[12]. Raw NGS data was analyzed by an in-house pipeline[12]. Experimental validation of *ACTN2* variants and segregation analysis were performed by PCR (primers available on request) and Sanger sequencing. *ACTN2* variants are described on transcript NM_001103.

A SNP genotyping (Illumina Infinium) was performed using the available DNAs from family 1 (III,1;III,4;III,6;IV,3;IV,4;IV,5;IV,6;IV,7;IV,8;IV,9;IV,10), family 2 (II,1;II,3;II,4;II,6;II,7;III,1;III,2) and family 3 (II,1).

A whole exome sequencing using SeqCap EZ MedExome (Roche, Basel, Switzerland) was performed on probands of family 1 (IV,2) and 3 (II,1) at the Finnish Institute of Molecular Medicine (FIMM) with Illumina HiSeq2500 system. Reads were aligned to the human reference genome (GRCh38/hg38) with the BWA[13], and a GATK standard pipeline was used for variant calling. Variants were then annotated using Annovar[14].

RNA from patient II,7 in family 2 was extracting with the RNeasy Plus Universal mini kit (QIAGEN, Hilden, Germany) according to the manufacturer's protocol._cDNA synthesis was performed with High Capacity cDNA Reverse Transcription kit (Applied Biosystems, Ghent, Belgium). RT-PCR was performed using primers designed with Primer3 software (available on request) and a Phusion High-Fidelity DNA Polymerase (Thermo Fisher Scientific, Madison, Wisconsin, USA).

Structure modelling

Human alpha-actinin2 was visualized in DeepView/Swiss-PdbViewer v 4.1.0 [15] and POV-Ray v. 3.7 (http://www.povray.org) using the structures 5A36[16] and 4D1E[9] from PDB.

Results

Clinical features

Family 1

Nine patients in two generations were clinically investigated. In addition three family members (II:1, II:2, III:4) were considered affected as they had similar distal weakness and walking difficulties, but were already deceased and not available for further studies (Fig 1). The mean age at symptom onset was 40.5 years (range 34-53 years). The presenting symptom was distal lower leg weakness especially with bilateral or one-sided foot drop in five of the patients. Two patients presented with myalgia while two patients were subjectively asymptomatic. Muscle weakness was predominant in the anterior compartment of the leg but, as the disease slowly progressed, the symptoms encompassed also posterior lower leg and proximal lower limb muscles. In the beginning of the disease, calf muscles and quadriceps could be asymmetrically hypertrophic and later became atrophic. Upper limb, trunk or facial muscles were not affected. EMG in the leg muscles mainly showed myopathic polyphasic brief and low amplitude potentials and early recruitment with some fibrillation and polyphasic larger amplitude potentials. One patient had ischemic heart disease and pacemaker; otherwise, none had cardiac or respiratory symptoms. One patient underwent Holter-ECG and echocardiography examination with normal results. CK values were variable ranging from normal to markedly elevated, up to 5000 UI/L. One patient presented as asymptomatic hyperckemia (1000-3000 U/L). The clinical details of the patients are shown in Table 1.

Family 2

The patients of family 2 presented with lower limb weakness between the ages of 41-63 years. In addition to distal lower leg weakness, the oldest patients of the family had severe proximal lower limb weakness. Two patients had asymmetrical involvement in the distal upper limbs (Table 1). Two patients were asymptomatic but on clinical examination were found to have hypertrophic quadriceps muscles and slightly elevated CK levels (233-249 IU/L, normal range 0-189 IU/L). One

of the two was also unable to walk on heels. The other patients had clearly elevated CK levels (400-1770 IU/L). EMG showed polyphasic, brief, low amplitude potentials with early recruitment in the leg muscles. Echocardiogram and Holter-ECG were normal in three patients studied.

Family 3

The father and son were the only affected members of family 3. The father had gait difficulties since the age of 60 years and on examination, he had asymmetric bilateral ankle dorsiflexion weakness with steppage gait. He also had proximal lower limb weakness causing difficulties rising from a chair. His son noticed muscle atrophy in both forearms more evident on the right at age 38. Wrist extensor weakness developed later. In addition, he had left ankle dorsiflexion weakness he had not been aware of. Both had the same mixed pattern on EMG as Family 1, and elevated CK levels (330-994 IU/L). Holter-ECG and echocardiogram of the son were normal. The father has been diagnosed of atrial flutter at the age of 73 years. Echocardiogram showed left ventricular hypertrophy.

Family 4

The father had distal lower limb weakness starting at age 45. Muscle weakness progressed to proximal lower limb muscles causing waddling and steppage gait. The daughter had a combination of proximal and distal lower limb weakness since aged 45 years. In addition, she had abdominal and neck flexor weakness. The father lost ambulation while the daughter uses two sticks for ambulation at the age of 62 years.

Muscle imaging

Muscle MRI or CT data were available in 15 patients. Imaging findings in each patient are listed in Table 1. The mildest cases showed fatty degenerative changes only in tibialis anterior muscles. In addition, frequently affected muscles were extensor digitorum longus, soleus and gastrocnemius

medialis (Fig. 2). With more advanced disease, fatty degeneration was severe in most thigh and usually also gluteal muscles. The observed pattern of involvement was similar between families with less severe findings in rectus femoris, gracilis, sartorius and semitendinosus (Fig. 2). Muscle imaging findings were asymmetric in most of the patients.

Muscle pathology

Muscle biopsy features varied from one case to another probably depending on the stage of the disease (Fig. 3). In the most severe cases there was prominent variation in the fiber size, increased numbers of internal nuclei and fibro-fatty tissue proliferation. Large numbers of fibers contained rimmed vacuoles. Moreover, some inclusion bodies were eosinophilic on HE stain and displayed congophilia. On oxidative reactions, there were major architectural changes with areas of myofibrillar disorganization and abundant lobulated fibers (Fig 3. A to E). ATPase reaction revealed type I predominance, and some myopathic type- grouping. No major protein aggregates were observed by using antibodies against desmin and myotilin except for very well defined inclusion bodies displaying p62 immunoreactivity and non-specific, diffuse desmin immunoreactivity in the atrophic fibers (data not shown). Immunofluorescence analysis revealed alpha-actinin enhancement in small atrophic fibers, and very occasional fibers containing small p62 and TDP-43 positive aggregates (Fig. 4).

Examination of a biopsy from a less affected individual revealed centrally located areas rounded or oval, that were hardly seen on HE stain, but were easily identified with PAS staining, and with oxidative reactions. These lesions displayed less intense oxidative activity than the surrounding area but were not devoid of oxidative activity, and therefore were not cores (Fig. 3 F to I).

Ultrastructural examination (Fig. 5) revealed severe myofibrillar abnormalities, with loss of normal striation pattern and thickening, duplication and fragmentation of the Z-lines. The majority of atrophic fibers showed a complete disorganization of the sarcomere structure that was replaced by remnants of filaments and fragments of Z-lines. There were autophagic vacuoles, and occasional cytoplasmic inclusions of 18 nm tubulofilaments. Additional utrastructural findings were electron-

dense inclusions surrounded by a clear halo resembling cytoplasmic bodies, core-like lesions, small areas of Z-line streaming, inclusions of electron-dense material of Z-disc origin and occasional honeycomb structures. Aberrant orientation of the myofibrils was the major abnormal finding in the sample showing the central lesions described above (Fig. 5 I).

Molecular genetics

We identified an *ACTN2* c.1459T>C (p.C487R) variant (Fig 1) in all the probands in families 1–3. In family 4, an *ACTN2* c.392T>C (p.L131P) variant was identified. These missense variants are both private (not listed in gnomAD[17] or in any other public database). Sanger sequencing, performed on the relatives for whom DNA was available, confirmed the co-segregation of the identified variants with the disease.

In family 4, the proband (II, 1) carried a truncating variant in titin gene (*TTN*; NM_133379:c.14454del:p.Ala4819Leufs*10) along with two further rare *TTN* missense variants. None of these *TTN* variants were identified in her affected father.

A linkage analysis in families 1, 2 and 3 showed a 1.8 Mb-long region (between rs34121575 at genomic position 2: 235181733 and rs6668721 at 2: 237127704) spanning *ACTN2*. WES analysis confirmed that the only rare (MAF<1% in gnomAD) exonic nonsynonymous variant shared by patient IV,2 in family 1 and patient II,1 in family 3 within the linked region was the *ACTN2* c.1459T>C (p.C487R) variant. Finally, a cDNA analysis demonstrated that the variant did not affect the splicing.

Discussion

Autosomal dominant distal myopathies with lower leg preponderance and rimmed vacuolar pathology with sarcomeric abnormalities are all within the differential diagnostic scope of this actininopathy. Clinically, this entity is characterized by adult-onset asymmetric weakness and atrophy of tibialis anterior muscle, slowly progressing to proximal muscles. In the first stages of the disease CK can be very high and calf or quadriceps hypertrophy present. Although *ACTN2* mutations have been associated with cardiomyopathy, our patients did not present cardiac involvement.

Alpha-actinin-2 is a protein highly expressed in the Z-disk of cardiac and skeletal sarcomeres, where it plays several structural and functional roles[7, 9, 10]. It connects the anti-parallel actin filaments to the sarcomeres and is an anchor for other Z-disk proteins. Through a number of interactions it is involved in signaling and mechanosensation[7-9, 18, 19].

Alpha-actinin-2 has a modular structure with an N-terminal actin-binding domain (ABD) containing 2 calponin homology domains (CH1 and CH2), a central rod domain with four spectrin-like repeats (SRs), and a C-terminal calmodulin-like domain (CAMD) composed of two hand motifs (EFs)[4, 9].

In a closed conformation, alpha-actinin-2 is an antiparallel homodimer, stabilized by interactions between the SRs[9].

In striated muscles, CAMD binds a specific hydrophobic alpha-actinin-binding motif located in titin z-repeats[8, 18]. The alpha-actinin interaction with titin and actin is highly dynamic and likely regulated by phospholipids as well as by complex intramolecular mechanisms[8, 9, 18]. The stable anchoring of the sarcomeric backbone titin within the Z-disk is provided by its interaction with alpha-actinin[18].

Interestingly, alpha-actinin-2 interacts with at least three other proteins involved in a distal myopathy: the aforementioned titin[8, 18], the UDP-N-acetylglucosamine 2-epimerase (GNE)[20], and the Z-disc-associated, Alternatively Spliced, PDZ Motif-containing Protein (ZASP)[21].

Considering the peculiar role of alpha-actinin-2 in skeletal muscle and its interactions with other clinically relevant proteins, *ACTN2* has been considered for a long time a strong candidate gene for skeletal muscle disorders. Nevertheless, *ACTN2* mutations have been linked for long time only to various cardiomyopathies such as HCM, DCM and other cardiac phenotypes[5, 6]. Two sporadic patients with a congenital core myopathy studied at the same time with our families and carrying two *ACTN2* variants in the fourth spectrin repeat have been just published[11].

In this study, we have described mutations in the *ACTN2* gene causing a late onset distal myopathy. In all the families enrolled, the private *ACTN2* variants are fully penetrant and perfectly co-segregate with the disease. Both variants are predicted to be causative by most of the bioinformatic programs currently in use (e.g. Polyphen[22] and Mutation Tester[23]). In particular, Cysteine 487 is a conserved amino acid located in the second spectrin repeat. The spectrin repeats are important for dimerization. In silico structural studies suggest that a mutation of this partially buried cysteine to the much larger, positively charged arginine could reduce the stability of this repeat and might indirectly interfere with dimerization (Fig 6).

Leucine 131 is in an α-helix in the first Calponin Homology (CH1) in the ABD domain. A mutation to proline will induce a kink in the helix and cause loss of the backbone H-bond to tryptophan 135. The interaction of tryptophan 135 with arginine 243 holds CH1 and CH2 together. The variant p.L131P probably destabilizes the structure, hampering a correct folding of the protein (Fig 6), which will need further studies.

Moreover, all our patients carrying *ACTN2* mutations share a very similar clinical phenotype, a characteristic pattern of muscle involvement by MRI and common histologic features.

The co-occurrence of the p.C487R variant in three families coming from the same village in northern Spain suggests that the three families may have a common ancestor through a founder, although no familial relationship is known. Most likely this *ACTN2* founder mutation will be identified in more patients from northern Spain with an adult-onset distal myopathy.

Our data demonstrates that *ACTN2* mutations cause a new type of dominant late-onset and slowly progressive distal myopathy. The wide spectrum of *ACTN2*-related clinical phenotypes probably reflects the observed high genetic heterogeneity and the complex network of interactions ACTN2 has with other sarcomeric proteins. The identification of additional patients with an *ACTN2*-related myopathy will probably improve the understanding of the genotype-phenotype correlation. Similarly, additional functional studies are needed to clarify and understand the molecular mechanisms of the disease leading to dystrophic loss of muscle tissue in the particular target muscles.

Acknowledgements

We acknowledge Merja Soininen for technical assistance, Meharji Arumilli for bioinformatics assistance and CSC – IT Center for Science Ltd. for providing computational resources.

M.S. is supported by a grant from the Magnus Ehrnrooth Foundation.

J. P. is supported by a grant from The Finnish Medical Foundation.

M.O. is supported by a grant from ISCIII PI14/00738, FEDER funds “a way to achieve Europe’’

P.H. is supported by the Erkko foundation and Liv&Hälsa foundation.

B.U. is supported by the Academy of Finland, the Sigrid Juselius foundation, the Erkko foundation, Finska läkaresällskapet and Liv&Hälsa foundations.

Author Contributions:

MS, JP, MO, PHJ, JS, FGB, JAU, PH and BU have contributed to the conception and design of the study.MS, JP, JJP, JW, MO, AMC, AV, PHJ, JS, FGB, JAU, PH and BU have contributed to the acquisition and analysis of data. MS, JP, MO, PHJ, and BU have contributed to drafting a significant portion of the manuscript or figures.

Potential Conflicts of Interest: The authors declare no conflicts of interest.

Figure 1: Pedigrees of the families enrolled in this study

DNA was collected from individuals marked with an asterisk *.

Figure 2: Muscle MRI

Milder form of involvement in patient F1 IV:3 shows affected tibialis anterior, extensor digitorum longus and gastrocnemius medialis muscles on the left. More advanced fatty degenerative changes are seen in patients F4 II:1 and F3 I:1 with large amount of thigh and leg muscles affected. Relatively spared muscles are rectus femoris, gracilis, sartorius and semitendinosus. At the distal leg tibialis anterior, soleus and gastrocnemius medialis are most frequently degenerated.

Figure 3: Histological findings

Muscle biopsy from patient F1 IV: 2 (A to E), showing variation in the fiber size, increased numbers of internal nuclei and fibro-fatty tissue proliferation (A), and rimmed vacuoles (A, B and D). Some fibers contain inclusion bodies eosinophilic on HE (B), and dark green (C) and displaying congophilia (D). NADH reaction showing lobulated fibers (E) Muscle biopsy from individual F1 IV: 7 (F to I) revealing variation in the fiber size, increased numbers of internal nuclei mild endomysial fibrosis. Note the presence of centrally located areas hardly seen on HE stain (F), but clearly revealed with PAS staining (G), and with oxidative reations (H). ATPase shows type I predominance, and some myopathic type- grouping (I).

Figure 4: Alpha-actinin immunolabeling

Patient F1 IV:2 Myotilin (green), alpha-actinin ACTN2/3 (red): alpha-actinin immunolabeling is enhanced in small atrophic fibers in the patient biopsy. p62 (green), TDP-43 (red): some fibers show small p62 and TDP-43 positive aggregates.

Figure 5: Ultrastructural features in actininopathy

(A) Focal disruption of sarcomere structure with streaming of Z-line spanning one sarcomere and emanation of electron-dense material. (B) Large area of sarcomeric disorganization and accumulation of dark material probably of Z-disk origin. (C to E) Severe loss of sarcomere structure with large areas or the totality of the muscle fiber replaced by fragmented sarcomeres, and

fragments of thickened Z-lines. (F) Electron-dense inclusions surrounded by a clear halo resembling cytoplasmic bodies. (G) Collections of 18 nm tubulofilaments (inset) within the cytoplasm of a muscle fiber. (H) Autophagic material and cellular debris. (I) Transversal section showing aberrant orientation of the myofibrils.

Figure 6: Positions of ACTN2 mutations

(A) The structure of the ABD domain of human ACTN2 (5a36.pdb) showing the location of Leu131 together with the residues important for CH1-CH2 binding (Trp135 and Arg243). Leu131 is interacting with residues in helix1 of CH1.

(B) Structure of the second spectrin domain of human ACTN2 (4d1e.pdb) showing the location of Cys487 and residues within 5 Å from the Cys487 side chain. Cys487 is in close proximity with residues in other alpha-helices in this domain

References

1. Udd B. Distal myopathies. Curr Neurol Neurosci Rep. 2014 Mar;14(3):434.
2. Milone M, Liewluck T. The Unfolding Spectrum of Inherited Distal Myopathies. Muscle Nerve. 2018 Aug 31.
3. Savarese M, Sarparanta J, Vihola A, Udd B, Hackman P. Increasing Role of Titin Mutations in Neuromuscular Disorders. J Neuromuscul Dis. 2016 Aug 30;3(3):293-308.
4. Beggs AH, Byers TJ, Knoll JH, Boyce FM, Bruns GA, Kunkel LM. Cloning and characterization of two human skeletal muscle alpha-actinin genes located on chromosomes 1 and 11. J Biol Chem. 1992 May 5;267(13):9281-8.
5. Mohapatra B, Jimenez S, Lin JH, et al. Mutations in the muscle LIM protein and alpha-actinin-2 genes in dilated cardiomyopathy and endocardial fibroelastosis. Mol Genet Metab. 2003 Sep-Oct;80(1-2):207-15.
6. Theis JL, Bos JM, Bartleson VB, et al. Echocardiographic-determined septal morphology in Z-disc hypertrophic cardiomyopathy. Biochem Biophys Res Commun. 2006 Dec 29;351(4):896-902.
7. Murphy AC, Young PW. The actinin family of actin cross-linking proteins - a genetic perspective. Cell Biosci. 2015;5:49.
8. Young P, Gautel M. The interaction of titin and alpha-actinin is controlled by a phospholipid-regulated intramolecular pseudoligand mechanism. EMBO J. 2000 Dec 1;19(23):6331-40.
9. Ribeiro Ede A, Jr., Pinotsis N, Ghisleni A, et al. The structure and regulation of human muscle alpha-actinin. Cell. 2014 Dec 4;159(6):1447-60.
10. Gupta V, Discenza M, Guyon JR, Kunkel LM, Beggs AH. alpha-Actinin-2 deficiency results in sarcomeric defects in zebrafish that cannot be rescued by alpha-actinin-3 revealing functional differences between sarcomeric isoforms. FASEB J. 2012 May;26(5):1892-908.
11. Lornage X, Romero NB, Grosgogeat CA, et al. ACTN2 mutations cause "Multiple structured Core Disease" (MsCD). Acta Neuropathol. 2019 Jan 30.
12. Evila A, Arumilli M, Udd B, Hackman P. Targeted next-generation sequencing assay for detection of mutations in primary myopathies. Neuromuscul Disord. 2016 Jan;26(1):7-15.
13. Li H, Durbin R. Fast and accurate short read alignment with Burrows-Wheeler transform. Bioinformatics. 2009 Jul 15;25(14):1754-60.
14. Yang H, Wang K. Genomic variant annotation and prioritization with ANNOVAR and wANNOVAR. Nat Protoc. 2015 Oct;10(10):1556-66.
15. Guex N, Peitsch MC. SWISS-MODEL and the Swiss-PdbViewer: an environment for comparative protein modeling. Electrophoresis. 1997 Dec;18(15):2714-23.
16. Haywood NJ, Wolny M, Rogers B, et al. Hypertrophic cardiomyopathy mutations in the calponin-homology domain of ACTN2 affect actin binding and cardiomyocyte Z-disc incorporation. Biochem J. 2016 Aug 15;473(16):2485-93.
17. Lek M, Karczewski KJ, Minikel EV, et al. Analysis of protein-coding genetic variation in 60,706 humans. Nature. 2016 Aug 18;536(7616):285-91.
18. Grison M, Merkel U, Kostan J, Djinovic-Carugo K, Rief M. alpha-Actinin/titin interaction: A dynamic and mechanically stable cluster of bonds in the muscle Z-disk. Proc Natl Acad Sci U S A. 2017 Jan 31;114(5):1015-20.
19. Martinelli VC, Kyle WB, Kojic S, et al. ZASP interacts with the mechanosensing protein Ankrd2 and p53 in the signalling network of striated muscle. PLoS One. 2014;9(3):e92259.
20. Harazi A, Becker-Cohen M, Zer H, Moshel O, Hinderlich S, Mitrani-Rosenbaum S. The Interaction of UDP-N-Acetylglucosamine 2-Epimerase/N-Acetylmannosamine Kinase (GNE) and Alpha-Actinin 2 Is Altered in GNE Myopathy M743T Mutant. Mol Neurobiol. 2017 May;54(4):2928-38.
21. Zhou Q, Ruiz-Lozano P, Martone ME, Chen J. Cypher, a striated muscle-restricted PDZ and LIM domain-containing protein, binds to alpha-actinin-2 and protein kinase C. J Biol Chem. 1999 Jul 9;274(28):19807-13.
22. Adzhubei IA, Schmidt S, Peshkin L, et al. A method and server for predicting damaging missense mutations. Nat Methods. 2010 Apr;7(4):248-9.

23. Schwarz JM, Cooper DN, Schuelke M, Seelow D. MutationTaster2: mutation prediction for the deep-sequencing age. Nat Methods. 2014 Apr;11(4):361-2.

Table 1 – Clinical details

Patient	Age at last exam/ sex	First symptoms/ age at onset	Muscle findings (MRC)	Muscle imaging	CK* UI/L
F1 III:1	77/F	Foot drop/ n.a.	Distal LL weakness and atrophy, posterior and anterior compartment, steppage gait on the left, right calf hypertrophy, ambulant with a walker	n.a.	382
F1 III:2	63/F	Left foot drop/ 53y	Ankle dorsifl L>R, mild gluteal weakness, absent tendon reflexes	Hamstrings (R>L), TA, EDL, Gmed, S	319
F1 III:3	57/F	Foot drop/ 37y	Ankle dorsifl (0/5, 1/5), right gastrocnemius	Hamstrings, VI, anterolateral and posterior lower leg (R>L)	531
F1 IV:2	37/M	Right calf pain/ 34y	Unable to walk on toes or heels, right side	S, Gmed, Glat, mild TA, mild hamstrings	5000
F1 IV:3	42/F	Unable to walk on toes/heels (left)/ n.a.	Distal atrophy on the left posterior and anterior compartment	TA (L), EDL (L), Gmed (L)	1648
F1 IV:4	34/F	Asymptomatic	Hypertrophic muscles, no weakness	TA (L>R)	485
F1 IV:5	43/F	Clumsy right foot/ 38y	Distal anterior compartment atrophy L>R, ankle dorsifl (3/5), peroneal (4/5, 3/5) calf hypertrophy, bilateral Achilles' tendon areflexia	n.a.	172
F1 IV:7	36/M	Asymptomatic	Calf hypertrophy	S (R>L), mild TA (R), anterior thigh (L>R)	1000-3000
F1 IV:10	47/F	Myalgia/ n.a.	No findings	Normal	147
F2 I:1	81/M	Lower limb weakness/ 63y	Hip extension (1/5), thigh abductors (2/5), thigh adductors (1/5), quadriceps (3-4/5, L>R), ischiotibial (2/5), ankle dorsifl and plantar fl (4/5)	Adductors, hamstrings, S, pectoral and paraspinal muscles	400-normal
F2 II:3	55/M	Right quadriceps atrophy/ 45y	Gluteal muscles, thigh adductors (2/5), hamstrings (4/5), ankle dorsifl (4/5, 3/5), left peroneal (3/5), left finger ext (4/5). Ambulant with waddling and steppage gait, hyperlordosis	Adductors, hamstrings, vastus intermedius, anterolateral lower leg, S	1646 - 897
F2 II:4	53/F	Asymptomatic	Quadriceps hypertrophy, ankle dorsifl (4/5), unable to walk on heels	TA	249
F2 II:5	46/M	Difficulties climbing stairs/ 41y	Right carpal radial extensors atrophy, anterior external compartment atrophy, calf hypertrophy, difficulties walking on toes	Gluteal, adductors (L), hamstrings, vastus intermedius, TA, S	1771 - 1407
F2 III:3	21/F	Asymptomatic	Quadriceps hypertrophy	Normal	233
F3 I:1	70/M	Gait difficulties/ 60y	Asymmetric bilateral weakness of tibialis anterior with steppage gait. Some difficulties to get up from a chair. Atrophy of anterior compartment of left leg	Gluteal and thigh muscles, S, TA, Gmed, peroneal	330
F3 II:1	43/M	Atrophy of extensor carpi radialis/ 38y	Wrist ext, left ankle dorsifl	TA (L), Gmed/lat (R)	994
F4 II:1	80/M	Distal lower leg weakness/ 45y	Foot drop, severe proximal LL (L>R), WCB	Gluteal, anterior thigh and hamstring muscles, anterolateral leg muscles (L>R), S, mild Gmed	Normal
F4 III:1	62/F	Right ankle dorsifl and proximal weakness/ 45y	Ankle dorsifl (R>L), proximal LL (hip/ knee ext), waddling gait, neck fl and abdominal. Ambulant with two sticks	n.a.	n.a.

BF, biceps femoris; CK, creatine kinase; EDL, extensor digitorum longus; F, female; Gmed, gastrocnemius medialis; Glat, gastrocnemius lateralis; L, left; LL, lower limbs; M, male; MRC, The Medical Research Council scale; n.a., not available, R, right; S, soleus; SM, semimembranosus; TA, tibialis anterior; UL, upper limbs; VI, vastus intermedius; WCB, wheelchair bound

*normal values for CK are 0-189 IU/L

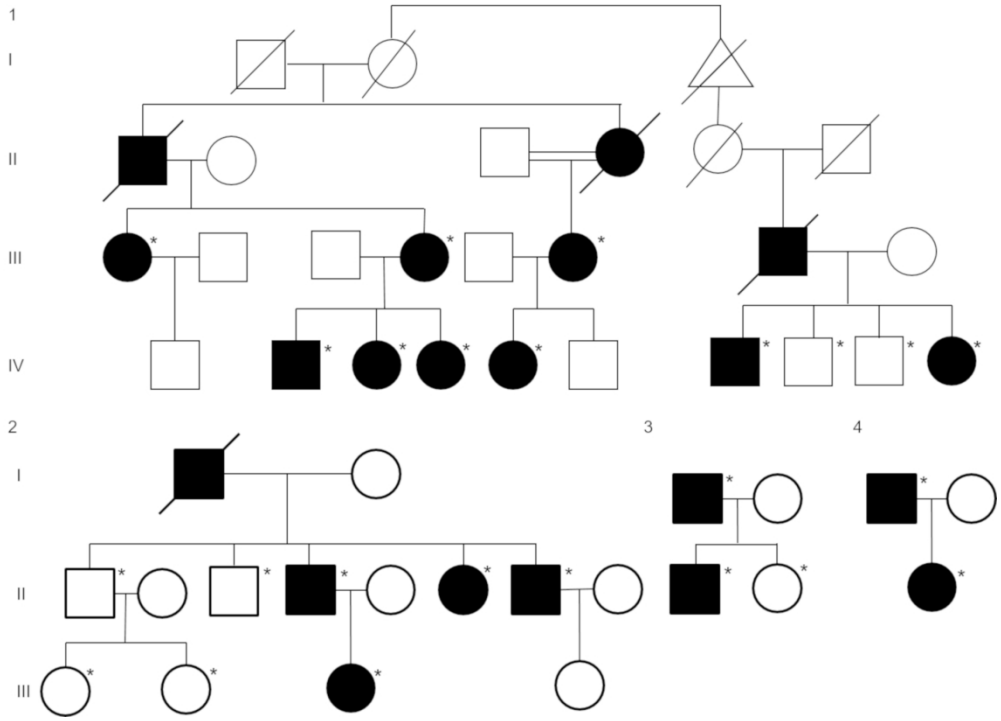

Figure 1: Pedigrees of the families enrolled in this study
DNA was collected from individuals marked with an asterisk *.

168x121mm (300 x 300 DPI)

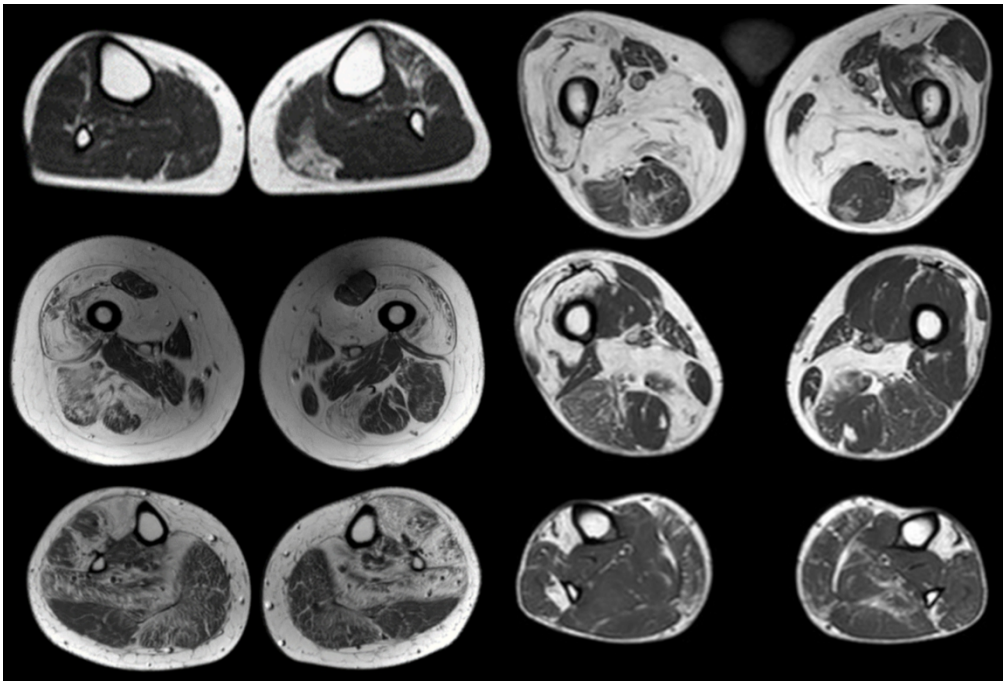

Figure 2: Muscle MRI
Milder form of involvement in patient F1 IV:3 shows affected tibialis anterior, extensor digitorum longus and gastrocnemius medialis muscles on the left. More advanced fatty degenerative changes are seen in patients F4 II:1 and F3 I:1 with large amount of thigh and leg muscles affected. Relatively spared muscles are rectus femoris, gracilis, sartorius and semitendinosus. At the distal leg tibialis anterior, soleus and gastrocnemius medialis are most frequently degenerated.

170x115mm (300 x 300 DPI)

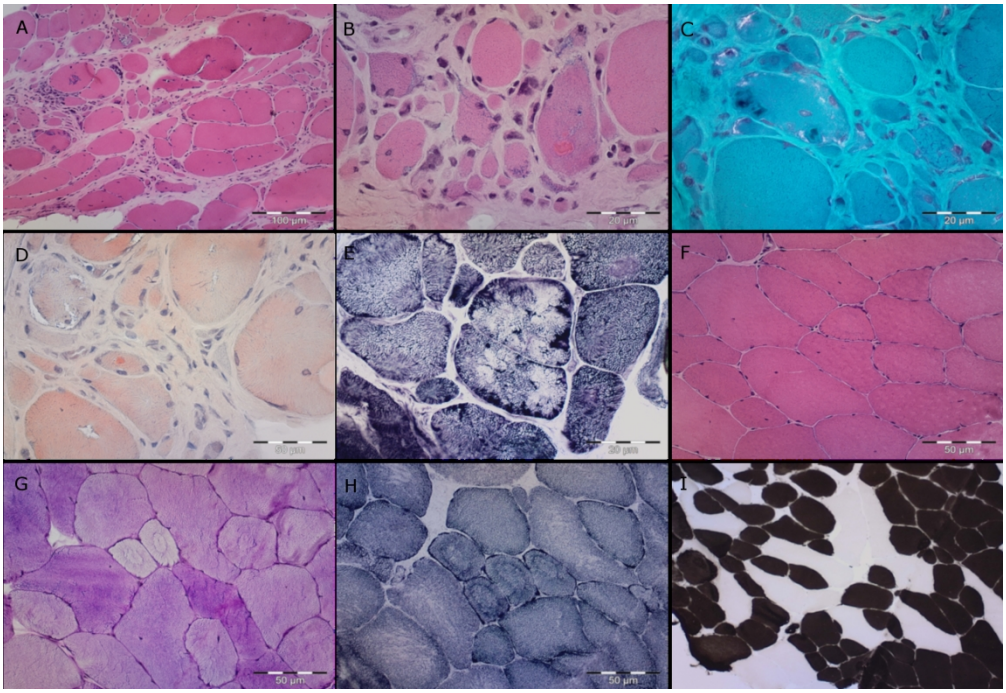

Figure 3: Histological findings
Muscle biopsy from patient F1 IV: 2 (A to E), showing variation in the fiber size, increased numbers of internal nuclei and fibro-fatty tissue proliferation (A), and rimmed vacuoles (A, B and D). Some fibers contain inclusion bodies eosinophilic on HE (B), and dark green (C) and displaying congophilia (D). NADH reaction showing lobulated fibers (E) Muscle biopsy from individual F1 IV: 7 (F to I) revealing variation in the fiber size, increased numbers of internal nuclei mild endomysial fibrosis. Note the presence of centrally located areas hardly seen on HE stain (F), but clearly revealed with PAS staining (G), and with oxidative reations (H). ATPase shows type I predominance, and some myopathic type- grouping (I).

180x123mm (300 x 300 DPI)

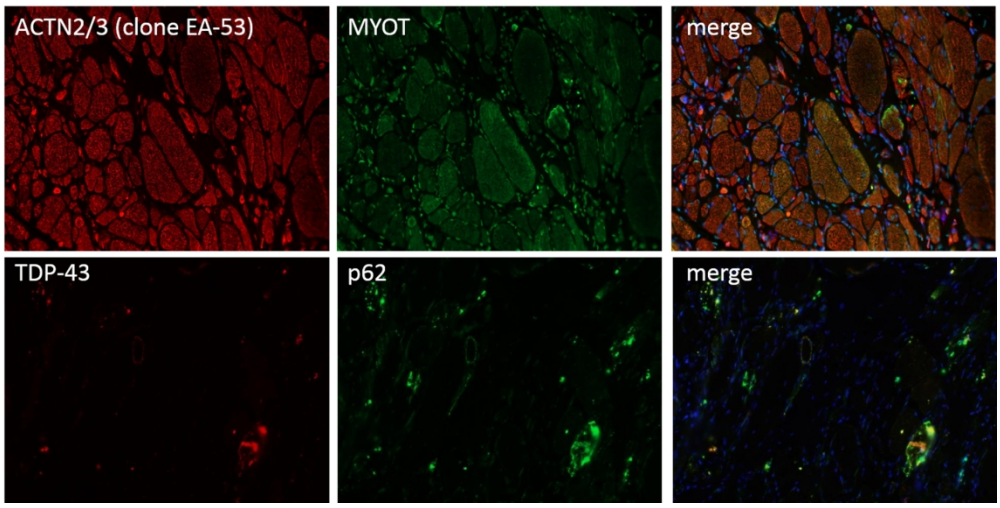

Figure 4: Alpha-actinin immunolabeling
Patient F1 IV:2 Myotilin (green), alpha-actinin ACTN2/3 (red): alpha-actinin immunolabeling is enhanced in small atrophic fibers in the patient biopsy. p62 (green), TDP-43 (red): some fibers show small p62 and TDP-43 positive aggregates.

169x85mm (300 x 300 DPI)

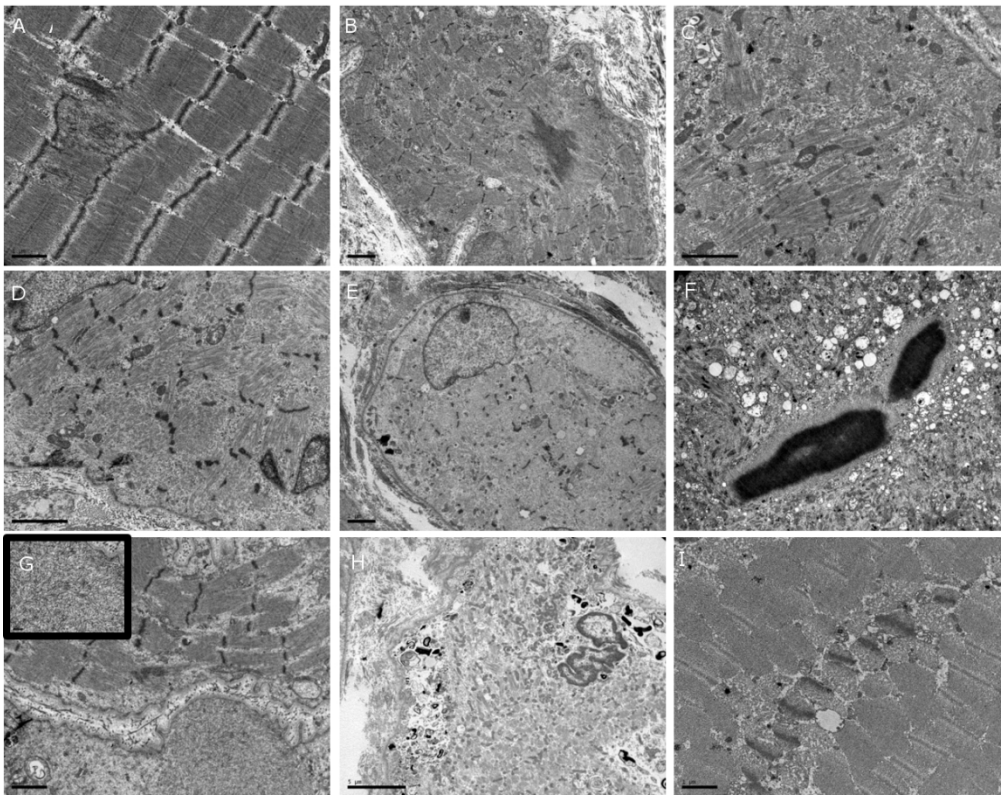

Figure 5: Ultrastructural features in actininopathy
(A) Focal disruption of sarcomere structure with streaming of Z-line spanning one sarcomere and emanation of electron-dense material. (B) Large area of sarcomeric disorganization and accumulation of dark material probably of Z-disk origin. (C to E) Severe loss of sarcomere structure with large areas or the totality of the muscle fiber replaced by fragmented sarcomeres, and fragments of thickened Z-lines. (F) Electron-dense inclusions surrounded by a clear halo resembling cytoplasmic bodies. (G) Collections of 18 nm tubulofilaments (inset) within the cytoplasm of a muscle fiber. (H) Autophagic material and cellular debris. (I) Transversal section showing aberrant orientation of the myofibrils.

169x134mm (187 x 187 DPI)

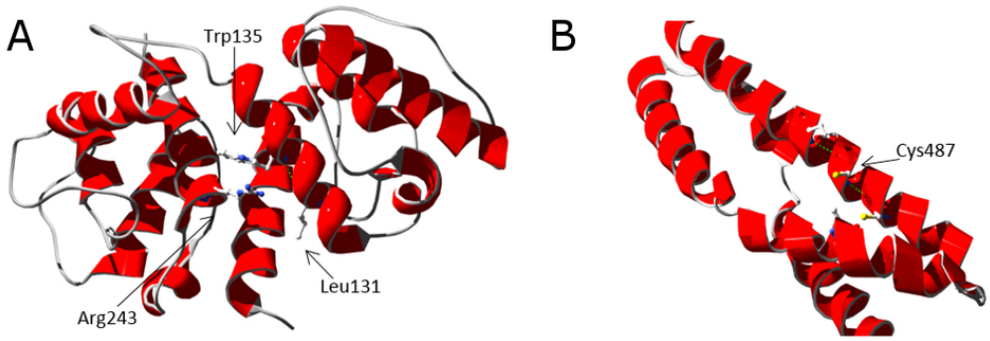

Figure 6: Positions of ACTN2 mutations
a) The structure of the ABD domain of human ACTN2 (5a36.pdb) showing the location of Leu131 together with the residues important for CH1-CH2 binding (Trp135 and Arg243). Leu131 is interacting with residues in helix1 of CH1.
b) Structure of the second spectrin domain of human ACTN2 (4d1e.pdb) showing the location of Cys487 and residues within 5 Å from the Cys487 side chain. Cys487 is in close proximity with residues in other alpha-helices in this domain.

79x27mm (300 x 300 DPI)